



Published in final edited form as:

Science. 2001 December 7; 294(5549): 2172–2175. doi:10.1126/science.1063224.

Central Role of the CNGA4 Channel Subunit in Ca²⁺-Calmodulin-Dependent Odor Adaptation

Steven D. Munger^{1,2,*}, Andrew P. Lane^{5,†}, Haining Zhong³, Trese Leinders-Zufall⁵, King-Wai Yau^{1,3,4}, Frank Zufall⁵, and Randall R. Reed^{1,2,3,‡}

¹ Howard Hughes Medical Institute, Johns Hopkins University School of Medicine, Baltimore, MD 21205, USA

² Department of Molecular Biology and Genetics, Johns Hopkins University School of Medicine, Baltimore, MD 21205, USA

³ Department of Neuroscience, Johns Hopkins University School of Medicine, Baltimore, MD 21205, USA

⁴ Department of Ophthalmology, Johns Hopkins University School of Medicine, Baltimore, MD 21205, USA

⁵ Department of Anatomy and Neurobiology and Program in Neuroscience, University of Maryland School of Medicine, Baltimore, MD 21201, USA

Abstract

Heteromultimeric cyclic nucleotide-gated (CNG) channels play a central role in the transduction of odorant signals and subsequent adaptation. The contributions of individual subunits to native channel function in olfactory receptor neurons remain unclear. Here, we show that the targeted deletion of the mouse *CNGA4* gene, which encodes a modulatory CNG subunit, results in a defect in odorant-dependent adaptation. Channels in excised membrane patches from the *CNGA4* null mouse exhibited slower Ca²⁺-calmodulin-mediated channel desensitization. Thus, the CNGA4 subunit accelerates the Ca²⁺-mediated negative feedback in olfactory signaling and allows rapid adaptation in this sensory system.

Olfactory receptor neurons (ORNs) respond to odorant stimulation with a receptor-mediated increase in intracellular cyclic adenosine 3',5'-monophosphate (cAMP), which directly activates a cyclic nucleotide-gated (CNG) channel in the plasma membrane (1). Calcium ions entering the cell through the open channel, in addition to contributing to the receptor potential (2,3), mediate cellular adaptation (4,5). A major mechanism for the rapid adaptation to odors is the Ca²⁺-calmodulin (Ca²⁺-CaM)-mediated desensitization of the CNG channel (6–10). Three CNG subunits are expressed in ORNs. One of these, CNGA2, is sufficient for generating a cyclic nucleotide-activated conductance and is a target for Ca²⁺-CaM-dependent desensitization in a heterologous expression system (6,7,11). Two other subunits, CNGA4 and CNGB1b, assemble with CNGA2 in the olfactory epithelium (12) and increase the nucleotide sensitivity of the CNGA2 subunit when coexpressed in vitro (12–15). The contributions of these modulatory subunits to odorant-induced responses in olfactory neurons have not been established.

[‡]To whom correspondence should be addressed. reed@jhmi.edu.

*Present address: Department of Anatomy and Neurobiology and Program in Neuroscience, University of Maryland School of Medicine, Baltimore, MD 21201, USA.

†Present address: Department of Otolaryngology, Johns Hopkins University School of Medicine, Baltimore, MD 21205, USA.

To define the role of the CNGA4 subunit in native olfactory function, we used gene targeting in embryonic stem cells to generate a mouse line functionally lacking this subunit (16). Exons coding for the CNGA4 pore region, two transmembrane domains, and the cyclic nucleotide-binding region (CNb) were deleted, as were three intervening introns (Fig. 1A), ensuring that no functional protein could be expressed (17). In situ hybridization experiments verified the presence of CNGA4 mRNA in ORNs of wild-type (+/+) and heterozygous (+/-) animals but not in null (-/-) mice (16) (Fig. 1B), demonstrating that the targeted deletion of the *CNGA4* gene abolished CNGA4 subunit expression.

Development of a normal olfactory system requires CNGA2-dependent neural activity (18–20). Because CNGA4 may itself form an ion channel insensitive to cyclic nucleotides but sensitive to other second messengers (21), we investigated whether CNGA4 might also be required for normal development of the olfactory epithelium and olfactory bulb. In situ hybridization studies showed that the olfactory marker protein mRNA (16) and protein (22), a signature of mature ORNs, was maintained in -/- mice, indicating that ORN development was not disrupted (22). The mRNA for major components of the transduction machinery was also normal, including CNGA2, CNGB1b, the heterotrimeric GTP-binding protein subunit $G\alpha_{olf}$, and the adenylyl cyclase ACIII (16,22). Tyrosine hydroxylase expression in the periglomerular cells of the olfactory bulb, a correlate of afferent activity (23), remained high in both CNGA4^{-/-} and wild-type animals (Fig. 1C), in contrast to expression in mice lacking CNGA2 (18). Therefore, we believe the CNGA4 subunit is not essential for normal development of the olfactory epithelium or bulb.

Heterologous expression studies have shown that homomeric channels formed by CNGA2 differ from the native olfactory channel with regard to several functional characteristics, including a much higher concentration of cAMP required for half-maximal ($K_{1/2}$) of the channel (12–15). The coexpression of CNGA2 with CNGA4 or CNGB1b, however, results in a cAMP $K_{1/2}$ value closer to that of the native channel, whereas the presence of all three subunits in the heterologous system further shifted the channel sensitivity to the native value. To assess the function of CNGA4 in the native channel, cAMP-activated currents were recorded in inside-out membrane patches excised from dendritic knobs of +/+, +/-, and -/- ORNs (16). Olfactory channels from the -/- animals exhibited a decreased affinity for cAMP, with a dose-response relation shifted by about 10-fold to higher cAMP concentrations; the behavior of the channels from +/- ORNs was like that of wild-type channels (Fig. 1, D and E). To determine whether this shift in channel sensitivity occurred as a change in the cell response, electro-olfactograms (EOGs) were recorded from +/+, +/-, and -/- mice (16) in response to a 500-ms pulse of isobutyl methyl xanthine (IBMX), which elevates intracellular cAMP by inhibiting endogenous phosphodiesterase activity (Fig. 1, F and G). The IBMX dose-response relations (24) for +/+ and +/- mice were essentially identical, but for -/- mice it was shifted by about threefold, to a higher IBMX concentration (Fig. 1G). The shift in the dose-response relation for -/- mice indicates that CNGA4 contributes to the high cAMP sensitivity of the native olfactory channel.

ORNs from CNGA4 null mice displayed an unanticipated defect in odor adaptation. Odor adaptation, a decrease in sensitivity arising from prolonged or prior odor exposure, was examined by eliciting an EOG from the olfactory epithelium. With an 8-s odor stimulus (cineole, 100 μ M), adaptation in +/+ mice was evident from the progressive reduction of the EOG response during the stimulus (Fig. 2A). The response phenotype in the CNGA4 -/- mice was different, in that the desensitization rate was reduced by about eightfold (Fig. 2, A and C). Application of IBMX at several subsaturating concentrations also caused a significant decrease in the desensitization rate (Fig. 2, B and C). This drastic difference in the speed of adaptation between wild-type and mutant mice was also observed in a paired-pulse paradigm (8,25). For CNGA4^{+/+} mice exposed to cineole (100 μ M, 500 ms), the peak amplitude of the EOG response

to the second stimulus (after a 3-s interstimulus interval) was only half that of the first (Fig. 2D). For *CNGA4*^{-/-} mice, on the other hand, the first and second responses were nearly identical. The same results were obtained with IBMX as a stimulus (Fig. 2, E and F). Hence, the presence of *CNGA4* in the native olfactory channel accelerates the adaptation of ORNs to odor stimulation.

The similarly altered adaptation kinetics between wild-type and *CNGA4*^{-/-} animals, regardless of whether odorant or IBMX was used as a stimulus, supports the notion that the underlying mechanism resides at the channel level, most likely in the form of Ca²⁺-mediated inhibition through calmodulin. Because the permeability of the heterologously expressed channel to Ca²⁺ is not significantly altered in the absence of *CNGA4* (26), we assessed whether *CNGA4* is necessary for the rapid binding of Ca²⁺-calmodulin to the channel complex. Exposure of excised membrane patches to 50 μM Ca²⁺ and 250 nM CaM produced broadly similar shifts in the dose-response relation between current activation and cAMP concentration for wild-type (4.3-fold) and *CNGA4*^{-/-} (3.0-fold) channels (Fig. 3A). This indicated that the steady-state modulation of the native olfactory channel by Ca²⁺-CaM does not require *CNGA4*, and this is consistent with previous work using heterologous expressions of the channel subunits (6,7,27). However, a large difference in the onset kinetics of the Ca²⁺-CaM modulation was observed. In excised-membrane-patch experiments (16), application of 50 μM Ca²⁺ and 1 μM CaM produced a rapid decrease in the cAMP-activated current for wild-type (Fig. 3B) and *CNGA4*^{+/-} channels (22). For *CNGA4*^{-/-} channels, however, the decrease in current by the same concentrations of Ca²⁺ and CaM was slowed by almost 70-fold (Fig. 3, C and D). The recovery of the current after removal of Ca²⁺ and CaM was severalfold faster for -/- than for +/+ channels (+/- channels were like those of wild-type animals) (Fig. 3E), suggesting that the presence of *CNGA4* also reduced to some degree the disinhibition rate when Ca²⁺ levels fell. The decelerated Ca²⁺-CaM-induced inhibition and the subsequent faster recovery may explain the adaptation defect manifested by the EOG of *CNGA4*^{-/-} animals in the long-pulse as well as the paired-pulse experiments; namely, the cAMP affinity of the *CNGA4*^{-/-} channel is much more resistant to change by the presence of Ca²⁺-CaM during odorant stimulation. In these experiments, we cannot resolve whether *CNGA4* alters the kinetics of Ca²⁺-CaM binding to the channel, the gating kinetics of the Ca²⁺-CaM-bound channel, or both. In heterologous expression where *CNGA4* is expressed, Ca²⁺-CaM binds to the channel equally well in the open or closed state; in the absence of *CNGA4*, Ca²⁺-CaM preferably binds to the channel in the closed state (28). Our results on the native channel are consistent with this observation.

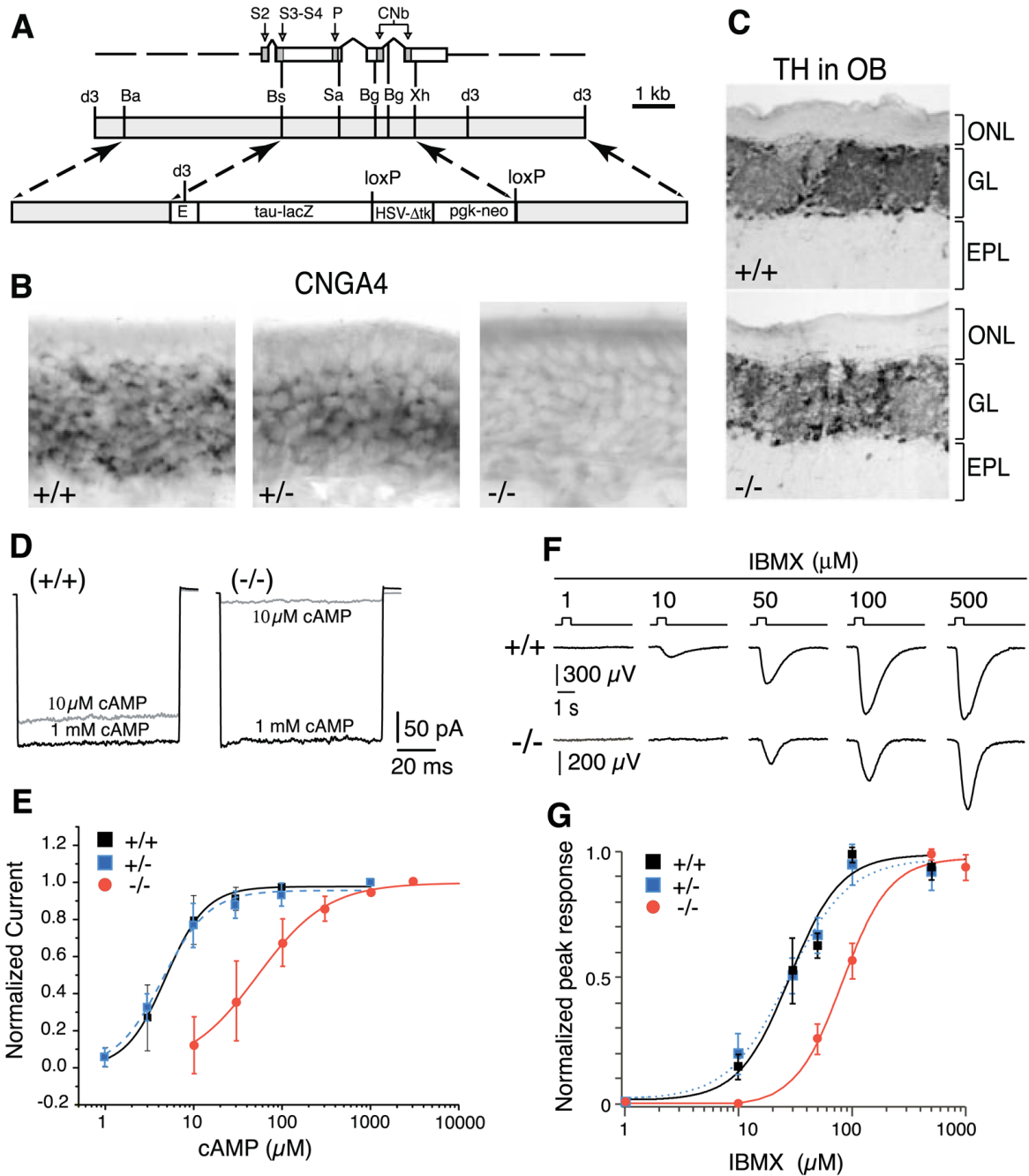
Our experiments using gene deletion demonstrate the importance of Ca²⁺-CaM-dependent channel modulation in the adaptation of native olfactory neurons to odorants, indicating the critical role of the *CNGA4* subunit in accelerating this adaptation. Thus far, among native CNG channels, only the olfactory channel is known to have three, instead of two, distinct subunits, including *CNGA4*. In correlation with this unique feature, the olfactory channel is also the only native CNG channel in which direct Ca²⁺-CaM modulation serves as a major negative feedback mechanism in signal transduction [unlike the situation in retinal photoreceptors (29)]. Rapid olfactory adaptation allows an animal to continually assess changes in odor environment and intensity that are essential to follow odor plumes and trails. The presence of *CNGA4* in the olfactory channel contributes to this feat.

Acknowledgments

We thank members of the Reed lab for helpful discussions, M. Cowan and the Johns Hopkins University Transgenic Facility for blastocyst injections and assistance in breeding mice, and Y. Wang for advice on embryonic stem cells. Supported by the Howard Hughes Medical Institute (S.D.M., R.R.R., and K.-W.Y.) and the National Institute on Deafness and Other Communication Disorders (NIDCD), the National Institute of Neurological Disorders and Stroke, and NSF (R.R.R., F.Z., and T.L.Z.). A.P.L. was the recipient of an NIDCD training grant.

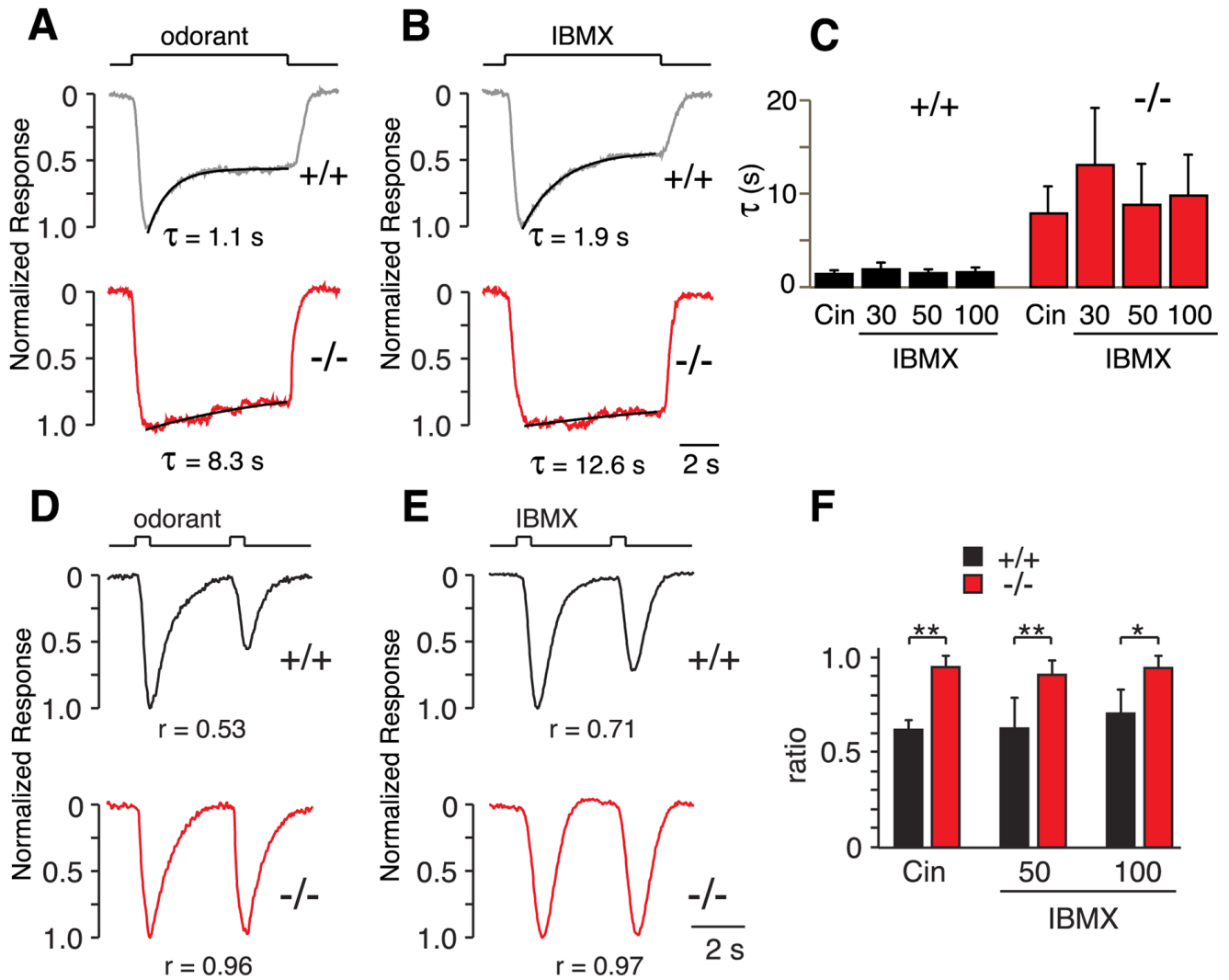
References and Notes

1. Different nomenclature has been under consideration in the field, and we and the Bradley group (28) have used a common nomenclature based on an informal survey of 20 colleagues in the field. Our discussion and proposal are described in a letter in this issue (www.sciencemag.org/cgi/content/summary/294/5549/2093a).
2. Menini A. *Curr Opin Neurobiol* 1999;9:419. [PubMed: 10448159]
3. Schild D, Restrepo D. *Physiol Rev* 1998;78:429. [PubMed: 9562035]
4. Zufall F, Leinders-Zufall T. *Chem Senses* 2000;25:473. [PubMed: 10944513]
5. Kurahashi T, Shibuya T. *Brain Res* 1990;515:261. [PubMed: 2113412]
6. Chen TY, Yau KW. *Nature* 1994;368:545. [PubMed: 7511217]
7. Liu M, Chen TY, Ahamed B, Li J, Yau KW. *Science* 1994;266:1348. [PubMed: 7526466]
8. Kurahashi T, Menini A. *Nature* 1997;385:725. [PubMed: 9034189]
9. Varnum MD, Zagotta WN. *Science* 1997;278:110. [PubMed: 9311913]
10. Grunwald ME, Yu WP, Yu HH, Yau KW. *J Biol Chem* 1998;273:9148. [PubMed: 9535905]
11. Dhallan RS, Yau KW, Schrader KA, Reed RR. *Nature* 1990;347:184. [PubMed: 1697649]
12. Bonigk W, et al. *J Neurosci* 1999;19:5332. [PubMed: 10377344]
13. Bradley J, Li J, Davidson N, Lester HA, Zinn K. *Proc Natl Acad Sci USA* 1994;91:8890. [PubMed: 7522325]
14. Liman ER, Buck LB. *Neuron* 1994;13:611. [PubMed: 7522482]
15. Sautter A, Zong X, Hofmann F, Biel M. *Proc Natl Acad Sci USA* 1998;95:4696. [PubMed: 9539801]
16. For supplementary data on the expression of transduction components, and for detailed methods, see *Science* Online at www.sciencemag.org/cgi/content/full/294/5549/2172/DC1.
17. β -galactosidase histochemistry of olfactory epithelium and the olfactory bulb revealed a faint but consistent expression pattern that only partially mimicked the native CNGA4 expression pattern. One explanation for this observation is that critical enhancer sequences were eliminated by the deletion and that reporter expression reflected the influence of nearby regulatory elements. The known presence of olfactory receptor genes in proximity to the CNGA4 gene might account for this zonal-restricted, scattered expression pattern observed in the olfactory epithelium (30).
18. Baker H, et al. *J Neurosci* 1999;19:9313. [PubMed: 10531436]
19. Zheng C, Feinstein P, Bozza T, Rodriguez I, Mombaerts P. *Neuron* 2000;26:81. [PubMed: 10798394]
20. Zhao H, Reed RR. *Cell* 2001;104:651. [PubMed: 11257220]
21. Broillet MC, Firestein S. *Neuron* 1997;18:951. [PubMed: 9208862]
22. Munger SD, et al. data not shown.
23. Baker H, Kawano T, Margolis FL, Joh TH. *J Neurosci* 1983;3:69. [PubMed: 6130133]
24. IBMX was used in these experiments because it induced responses in all olfactory cilia; useful dose-response relationships could not be determined for odors because saturation was never effectively achieved. These EOG measurements cannot be compared quantitatively with the excised-patch experiments because the EOG represents the contributions of both the CNG and a Ca^{2+} -gated Cl^- conductance in these cells.
25. Leinders-Zufall T, Greer CA, Shepherd GM, Zufall F. *J Neurosci* 1998;18:5630. [PubMed: 9671654]
26. Dzeja C, Hagen V, Kaupp UB, Frings S. *EMBO J* 1999;18:131. [PubMed: 9878057]
27. For unclear reasons, the shift in the cAMP dose-response relation observed here due to Ca^{2+} -CaM was smaller than previously reported (6).
28. Bradley J, Reuter D, Frings S. *Science* 2001;294:2176. [PubMed: 11739960]
29. Koutalos Y, Yau KW. *Trends Neurosci* 1996;19:73. [PubMed: 8820871]
30. Munger SD, Reed RR. unpublished data.

**Fig. 1.**

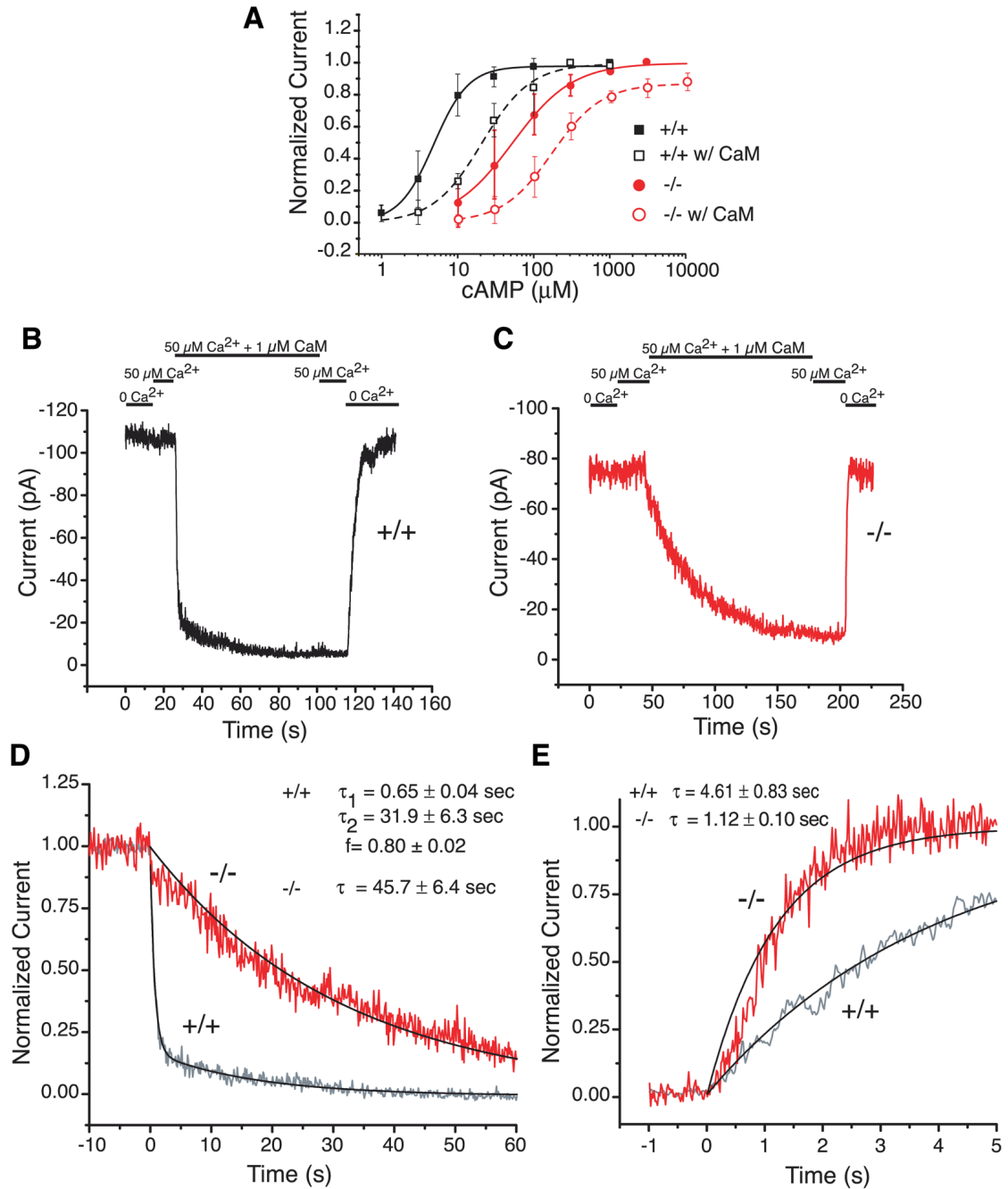
Targeted disruption of the *CNGA4* gene abolishes *CNGA4* expression and shifts the cyclic nucleotide sensitivity of the native CNG channel. (A) Exon-intron structure of the targeted region of the *CNGA4* gene (top), restriction map of the wild-type locus (middle), and targeting vector (bottom). S2, S3, and S4, transmembrane domains 2, 3, and 4; P, channel pore; CNb, cyclic nucleotide-binding domain; d3, Hind III; Bs, Bsi EI; Sa, Sac I; Bg, Bgl II; Xh, Xho I. The proper gene targeting of this locus was confirmed by Southern blot hybridization (22). (B) In situ hybridization with *CNGA4* probe on OE from *CNGA4* $+/+$, $+/-$, and $-/-$ mice. (C) Tyrosine hydroxylase immunohistochemistry (16) on sections of olfactory bulb from *CNGA4* $+/+$ and $-/-$ mice. Signal is observed in the glomerular layer (GL) and absent from

the outer nerve layer (ONL) and the external plexiform layer (EPL). **(D)** Currents induced by 1 mM and 10 μ M cAMP, respectively, from an excised, inside-out membrane patch from the dendritic knob of a +/+ (left) and a -/- ORN (right). Buffered zero- Ca^{2+} , Mg^{2+} Tyrode's solution was present on both sides of membrane. In each trace, the current is activated by a 90-ms voltage step from 0 to -60 mV. Data represent the average of 10 sequential voltage steps. **(E)** The cAMP dose response relationships after averaging and normalization for channels from +/+, +/-, and -/- mice. +/+ : one mouse, three patches; +/- : two mice, four patches; -/- : two mice, six patches. Error bars represent SEM. Smooth curves are fits by the Hill equation, with $K_{1/2}$ values and Hill coefficients of 4.9 μ M, 1.91 (+/+); 4.5 μ M, 1.66 (+/-); and 55.2 μ M, 1.10 (-/-), respectively. **(F)** EOG responses measured from the ciliary layer of a +/+ and a -/- OE. Stimulus was a single 500-ms pulse of IBMX at the indicated concentrations (in μ M) ejected from a multibarrel pipette. Maximum responses from the two kinds of animals were not significantly different (mean \pm SD = 655 \pm 165 μ V for +/+ and 593 \pm 267 μ V for -/-; more than six measurements were taken from four or five mice in each case). **(G)** Averaged and normalized IBMX dose-response relations from +/+ (solid squares), +/- (open squares, dashed blue line), and -/- (solid circles, red line) mice. Error bars represent SD. Smooth curves are fit by the Hill equation, with $K_{1/2}$ value and Hill coefficient of 28.3 μ M, 1.9 (+/+); 27.2 μ M, 1.7 (+/-); and 82.4 μ M, 2.0 (-/-), respectively.

**Fig. 2.**

CNGA4 $-/-$ olfactory receptor neurons exhibit a defect in adaptation. (A and B) Representative EOG responses to an 8-s pulse of (A) cineole or (B) IBMX. 100 μ M cineole was used to stimulate both $+/+$ and $-/-$ OE, whereas 50 μ M and 100 μ M IBMX were used for $+/+$ and $-/-$ OE, respectively. At these stimulus concentrations, none of the responses reached saturation. Fits are single-exponential decays with the indicated time constants. (C) Histograms showing collected results (mean \pm SD) from $+/+$ and $-/-$ mice. Three $+/+$ animals were treated with the following: cineole, time constant (τ) = 1.4 \pm 0.4 s (100 μ M, 10 independent measurements); IBMX, τ = 1.9 \pm 0.7 s (30 μ M, three independent measurements), 1.5 \pm 0.4 s (50 μ M, 11 independent measurements) and 1.6 \pm 0.5 s (100 μ M, three independent measurements), respectively. τ is significantly increased in the $-/-$ OE [Fisher's least significant difference (LSD) test: $P < 0.0001$]. Five $-/-$ animals were treated with the following: cineole, τ = 7.9 \pm 2.9 μ M s (seven independent measurements); IBMX, τ = 13.1 \pm 6.1 s (30 μ M, three independent measurements), 8.8 \pm 4.4 s (50 μ M, nine independent measurements) and 9.8 \pm 4.4 s (100 μ M, 10), respectively. (D and E) Representative EOG responses to paired 500-ms pulses of (D) cineole or (E) IBMX, delivered with a 3-s interstimulus interval. 100 μ M cineole was used to stimulate both $+/+$ and $-/-$ ORNs, whereas 50 μ M and 100 μ M IBMX was used for $+/+$ and $-/-$ animals, respectively. The peak amplitude ratio (r) between the first and second responses

is indicated at the bottom of each panel. **(F)** Collected results on the peak amplitude ratio, all measured at a 3-s interstimulus interval. For treatment with cineole, $r = 0.62 \pm 0.05$ (mean \pm SD, $n = 3$) for $+/+$ and 0.95 ± 0.06 ($n = 5$) for $-/-$ mice; $**P < 0.0001$, Fisher's LSD test. For treatment with 50 μM IBMX, $r = 0.62 \pm 0.17$ ($n = 4$) for $+/+$ and 0.91 ± 0.07 ($n = 8$) for $-/-$ mice; $**P < 0.0001$. For treatment with 100 μM IBMX, $r = 0.7 \pm 0.13$ ($n = 3$) for $+/+$ and 0.94 ± 0.07 ($n = 7$) for $-/-$ mice; $*P < 0.001$.

**Fig. 3.**

The onset kinetics of inhibition by Ca^{2+} -CaM are dramatically altered for CNGA4 $-/-$ channels. **(A)** The steady-state cAMP dose-response relations for CNGA4 $+/+$ and $-/-$ channels were comparably shifted by 50 μM Ca^{2+} and 250 nM CaM. These collected results are from the same patches as those in Fig. 1E. The $K_{1/2}$ value and Hill coefficient fit to the collected results in the presence of Ca^{2+} -CaM are 20.7 μM , 1.35 for $+/+$; and 169.8 μM , 1.34 for $-/-$ channels, respectively. Although not shown in the figure, the data for $+/-$ channels are 20.5 μM , 1.48. The $K_{1/2}$ value and Hill coefficient in the absence of Ca^{2+} -CaM are indicated in the legend to Fig. 1E. **(B and C)** There is a large difference in the kinetics of inhibition of **(B)** $+/+$ and **(C)** $-/-$ channels. Step applications of solutions containing 0 Ca^{2+} plus 50 μM Ca^{2+} and

50 μM Ca^{2+} plus 1 μM CaM are indicated by bars (16). The chosen cAMP concentrations, (B) 7.5 μM cAMP and (C) 75 μM cAMP, corresponded to a concentration 1.5 times the $K_{1/2}$ of the respective channels. Membrane voltage was steadily held at -30 mV for both. (D and E) The onset kinetics of inhibition of $+/+$ and $-/-$ channels are compared at a higher time resolution. The same traces are shown as in (B) and (C). Fits (16) are $\tau_1 = 0.72$ s, $\tau_2 = 16.8$ s; $f = 0.82$ for $+/+$ and $\tau = 31.4$ s for $-/-$ channels. A small fast component in the $-/-$ channel was not observed in every experiment and was ignored in the curve fit. Collected time constants and f values from all experiments are as indicated in the figure. Although not shown, CNGA4 $+/-$ channels behaved like those of wild-type animals, with $\tau_1 = 0.77 \pm 0.13$ s, $\tau_2 = 37.2 \pm 11.1$ s, and $f = 0.83 \pm 0.04$ (mean \pm SEM). Altogether, nine patches from three $+/+$ mice, nine patches from three $+/-$ mice, and eight patches from four $-/-$ mice were tested. (E) Similar plot as in (D), but for the recovery kinetics after removal of Ca^{2+} -CaM. Fits are single exponentials, with $\tau = 3.91$ s for $+/+$ and 1.19 s for $-/-$ channels. Collected data are as indicated in the figure. Although not shown, $+/-$ channels behaved like those of wild-type animals, with $\tau = 3.97 \pm 0.44$ s.